Application of Mesoporous Silica Containing Benzotriazole in Epoxy Coating Applied to Plain Carbon Steel and Study of Its Corrosion Behavior

Mahdi Yeganeh [1,*], Mahdi Omidi [2], Arash Etemed [3], Mohammad Reza Rostami [4], Mohammad Esmaeil Shafiei [2]

[1] *Department of Materials Science and Engineering, Faculty of Engineering, Shahid Chamran University of Ahvaz, Ahvaz, Iran.*
[2] *Advanced Materials Research Center, Department of Materials Engineering, Najafabad Branch, Islamic Azad University, Najafabad, Iran.*
[3] *Nanomaterial Engineering, Isfahan University, Isfahan, Iran.*
[4] *Master of Science Student, Nano Materials Engineering, University of Science and Technology, Tehran, Iran.*

ARTICLE INFO

Article history:

Received 7 June 2018
Accepted 17 July 2018
Available online 5 November 2018

Keywords:
Mesoporous silica
Corrosion
Epoxy coating
Benzotriazole

ABSTRACT

The idea of smart inhibitors is based on the principle that an inhibitor is used where needed. This will reduce the use of inhibitors and protect materials in hostile environments. On the other hand, direct addition of the inhibitor within the coating can be harmful, resulting in the loss of inhibitors ability, deterioration in the coating or both of them. An appropriate method for solving these problems is the use of neutral host systems that act as a nanocontainer system or reservoir and are filled with arbitrary inhibitor. In this study, mesoporous silica with and without corrosion inhibitor (benzotriazole) were dispersed within an epoxy coating to protect the steel sheet. Then, the corrosion properties of these coatings with and without mesoporous silica particles were compared in a saline solution. Electrochemical studies showed that coatings containing particles could protect the surface of steel in the chloride environment. The impedance modulus ($Z_{100\ mHz}$) and corrosion resistance (R_{corr}) regarding the coating embedded with mesoporous silica doped with inhibitor showed a value about one order of magnitude higher than that of a coating without inhibitor. This behavior could be due to the release of benzotriazole at the interface of the epoxy coating. In addition, the scratched coating with mesoporous silica doped with inhibitor exhibited less corrosion products compared to the coating without inhibitor which also confirmed the release of benzotriazole on demand of the corrosion process.

1-Introduction

The application of corrosion inhibitors in coatings in a variety of environments has faced two major challenges including the reaction of inhibitor with the coating and loss of system efficiency, and the use of inhibitor. Smart inhibition systems are designed to prevent both unwanted reactions and use the inhibitor where needed. To overcome these problems, several solutions have been proposed based on the use of inhibitory reservoirs, which prevents the interaction of the inhibitor and the matrix. These reservoirs include micro and nano capsules [1-2], nanotubes [3], ion exchanger particles [4-7] and layer by layer polyelectrolytes [8-9]. In these reservoirs, an ionic exchange may occur

* Corresponding author:
E-mail address: m.yeganeh@scu.ac.ir

between the corrosive ion and the inhibitor inside the system, or the inhibitor can be released by changing the pH in the corrosion region or prevent the corrosion by long-term penetration from inside of the system. In this study, the nanocontainer particles which are known as mesoporous silica have been used. The mesoporous silica has hexagonal structure with uniform pores with the diameter of about 2 to 50 nm. The specific surface area and volume of the cavities in these materials are about 700-1500 m^2/g and 1 cm^3/g respectively. They also have good chemical and thermal stability and can be simply functionalized [10]. These materials have found many applications in the field of adsorption [11], filtration [12], storage [13], release [14], catalyst [15], chemical separation [16], drug delivery [17] and electronic devices [18]. Recently, these materials are used to control corrosion damages. Borisova et al. doped the benzotriazole into these materials and inoculated the material into sol-gel films. The corrosion resistance of these coatings was improved in comparison to the typical sol-gel coating. The results of their research also showed that the inhibitor release depends on the pH value [19, 20]. In our previous research, the effect of doped molybdate inhibitor inside the mesoporous silica on steel corrosion control was investigated. It was found that the controlled release of molybdate in addition to reducing the corrosion rate also results in self-healing of the surface [21]. In this study, mesoporous silica was used as a nanocontainer corrosion inhibitor of benzotriazole in the corrosive environment. Composites including mesoporous silica containing inhibitor + resin, mesoporous silica without inhibitor + resin were prepared and applied on a steel substrate. Then, the effect of mesoporous silica particles containing benzotriazole on corrosion behavior of steel was investigated.

2- Materials and methods

Mesoporous silica particle containing inhibitor is obtained by the combination of a surfactant material (Hexadecyltrimethylammonium bromide) with tetraethyl orthosilicate precursor in an acidic environment [21]. The size of the pores, the diameter of mesoporous silica and their morphology were investigated by transmission electron microscopy (300 kV) and scanning electron microscopy. The specific area of the pores, the mean diameter of the pores and the volume of the pores were calculated by the adsorption-desorption isotherm method. The mesoporous silica was functionalized by silane groups of equal weight ratios in toluene for 3 hours. Then the powders were filtered by ethanol. In the next step, iron (III) chloride was added to the functionalized mesoporous silica. The iron ion adsorption was carried out at ambient temperature and propanol atmosphere for 3 hours and the weight ratio equal to that of mesoporous silica. The obtained powder denoted as MS. Finally, the benzotriazole corrosion inhibitor was mixed with the mesoporous silica material of the previous steps by weight ratio of 1/2 in aqueous solution for 1 day. This powder denoted as MSInh. The specific surface area was calculated with absorption data at low pressure and using Brunauer–Emmett–Teller (BET) method. The mean diameter and mean volume of the cavities were calculated by the desorption branch using Bart-Joiner-Holland method. The crystallography of the mesoporous silica structure was performed by X-Perth diffractometer in the range of 1-7 °.

In order to make the coating, 1001 diluted epoxy resin with a solid content of 75% and weight equals to 450-550 with hardener were used. The steel substrate prior to coating was polished with silicon carbide sand papers of 80 to 1000 # and then immersed into a 10 wt. % KOH solution for 10 min at ambient temperature and then washed with acetone and dried. In order to prepare the coating mixture, first the epoxy and mesoporous silica powder were mixed for 30 min and then homogenized with ultrasonic probes for 1 h. In the next step, by applying the hardener to the above mixture, the mixing operation was performed 30 min in a mixer. Then the epoxy composite coating containing 1 wt. % of nanocontainer particles was applied to the surface with 50 μm thickness using a film-applicator. The coatings were then cured in a furnace at 50-55 °C for 4 h. Finally, two types of coatings epoxy containing mesoporous silica with and without inhibitor were produced and their properties were investigated.

Electrochemical impedance test was performed on the coatings in comparison with the coating

without inhibitor. In order to determine the corrosion resistance of the coatings, the specimens were placed in 100 cc of 0.03 M saline solution for 1, 7 and 10 days and then an electrochemical impedance test was performed considering the calomel electrode as the reference electrode and platinum electrode was used as a counter electrode in the potentiostat circuit. It took about 20 to 60 min for the open circuit potential to be stable. The frequency range was changed from 100 kHz to 10 mHz around the open circuit potential of the samples. The applied sinusoidal wave had a voltage of 5 mV. The equivalent circuit simulation program (ZView 3.1c) was used for equivalent circuit fitting and experimental data analysis. In order to ensure the repeatability, the corrosion tests were performed at least twice.

3- Results and discussion

Figure 1 (a) and (b) show respectively the SEM and TEM images of the obtained mesoporous silica. As can be seen, the diameter of the mesoporous silica tubes varies from 50 to 300 nm, while the TEM image shows a diameter of about 4-5 nm for each of the pore of this material. The size of the observed pores in the TEM image shows the mesoporous structure of the synthesized material [21, 22].

Figure 2 shows the X-ray diffraction pattern of the mesoporous silica. The peak (100) is located at 2θ =2.05°, which according to Bragg's relationship the plane distances will be calculated by 4.4 nm and agree with the results of transmitted electron microscopic images.

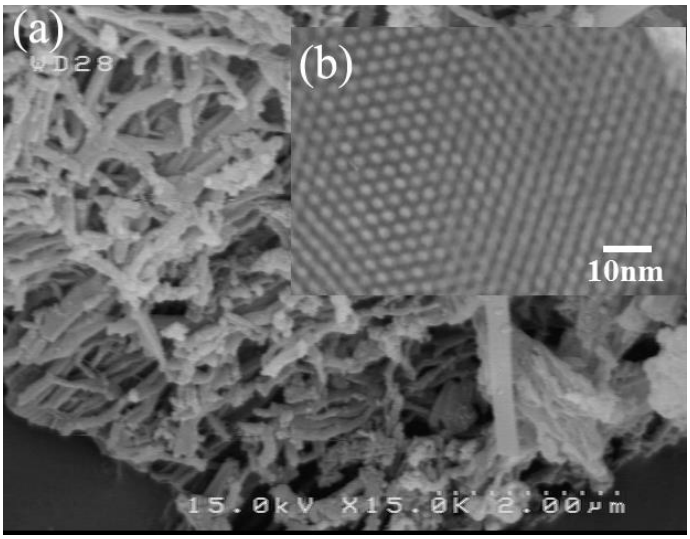

Fig. 1. (a) SEM image and (b) TEM image of mesoporous silica [21].

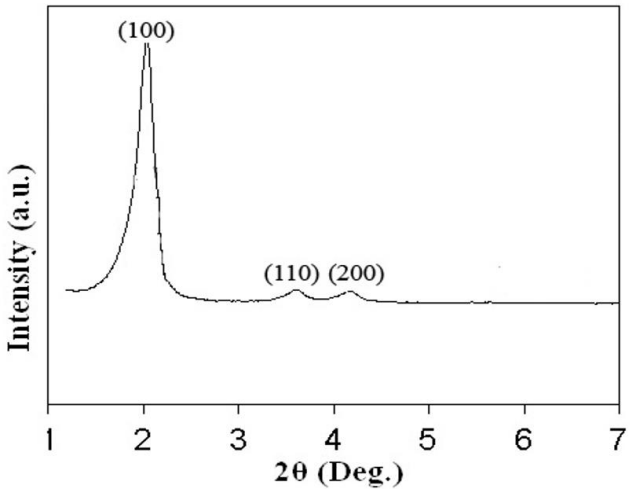

Fig. 2. XRD pattern of mesoporous silica [21].

In order to functionalize the mesoporous silica, the silane group was first added to the surface of them (Figure 3). The general reaction of the mesoporous silica surface (with OH surface graft) and the functional group can be written as equation (1) [23]:

$$Si\text{-}OH + R'O\text{-}SiR_3 \rightarrow \equiv Si\text{-}OSiR_3 + HOR' \quad (1)\equiv$$

In the next step after functionalizing, $FeCl_3$ (a material with the ability to form cation on the surface) is used to create an intermediate material on this system. Then in the final step, the inhibitory composition can enter the system with an electrostatic bond which is a weak bond and react with iron cation.

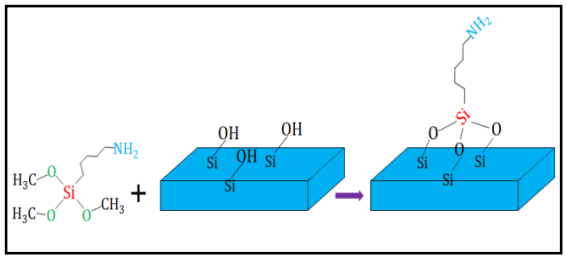

Fig. 3. An overview of the functionalizing process of mesoporous silica.

The structure of benzotriazole is organic, but due to the charge density in its nitrogenous part, it is expected to have polar behavior. The benzotriazole structure is shown in Figure 4. This inhibitor in spite of dissolution in water will have a negative charge in the nitrogenous end and will lose its proton, and by this free nitrogen end and sharing its free single electron can be absorbed onto the iron surface. The presence of a link between the iron orbital (d) and the π electron of benzotriazole inhibitor is also effective in this absorption. By the absorption of this molecular, a layer is formed on the surface which in the presence of chloride ion in solution, its composition is $[Fe_n(Cl)_p(BTA)_m]$, which relatively prevents the solution to reach the surface [24].

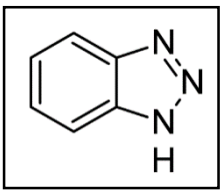

Fig. 4. Chemical structure of benzotriazole.

Figure 5 shows the fourier-transform infrared spectroscopy (FT-IR) spectra of the powders containing benzotriazole in compared to the mesoporous silica powders prior to the application of the inhibitor. For the mesoporous silica (MS), the bands at 3395 and 1604 cm^{-1} were associated to the stretching (3395 cm^{-1}) and the bending (1604 cm^{-1}) vibrations of the surface silanol groups or the remaining adsorbed water molecules. The typical Si-O-Si bands around 1080, 795 and 455 cm^{-1} were associated with the formation of a condensed silica network. MS exhibited some peaks related to the functionalization of mesoporous silica. The most distinct peak regarding the functionalization process was related to the NH adsorption. MS showed the original bands for C-H stretching at around 2792 cm^{-1}, N-H bending vibration around 678 cm^{-1}, and -NH- deformation vibration around 1450 cm^{-1}[25-26]. In the case of MSInh, the most important phenomenon observed in these diagrams is the decrease in peak intensity of the silica structure and increasing NH bonds, which can occur as a result of the absorption of benzotriazole.

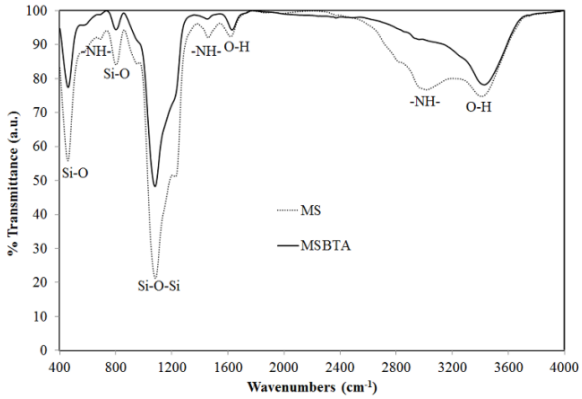

Fig. 5. Fourier-transform infrared spectroscopy spectra of mesoporous silica with and without benzotriazole inhibitor.

Figure 6 shows the adsorption/desorption diagram of the mesoporous silica powder containing benzotriazole (MSInh) as compared to the mesoporous silica powder (MS). This curve is somewhat similar to the isotherm type 4, the first part of the curve showing a single-layer absorption, a low gradient in the middle region indicating multi-layered adsorption and the desorption curve representing capillary condensation [27] . The type of the diagram

represents the mesoporous structure of the substance after absorption of benzotriazole. But the difference with the regular curve of mesoporous silica indicates a pseudo-cylindrical (irregular) structure after absorption of the inhibitor [27]. The values of the specific surface area, the pore volume, and the average pore diameter of the mesoporous silica were obtained 776.2 $m^2 g^{-1}$, 0.84 $cm^3 g^{-1}$, and 4.23 nm, respectively. These corresponding parameters for MSInh were obtained 539 $m^2 g^{-1}$, 0.61 $m^3 g^{-1}$ and 3.8 nm, respectively. As it can be seen, with the introduction of benzotriazole into the mesoporous silica structure, the specific surface, volume and radius of the pores decrease which indicate the absorption of the inhibitor on the surface.

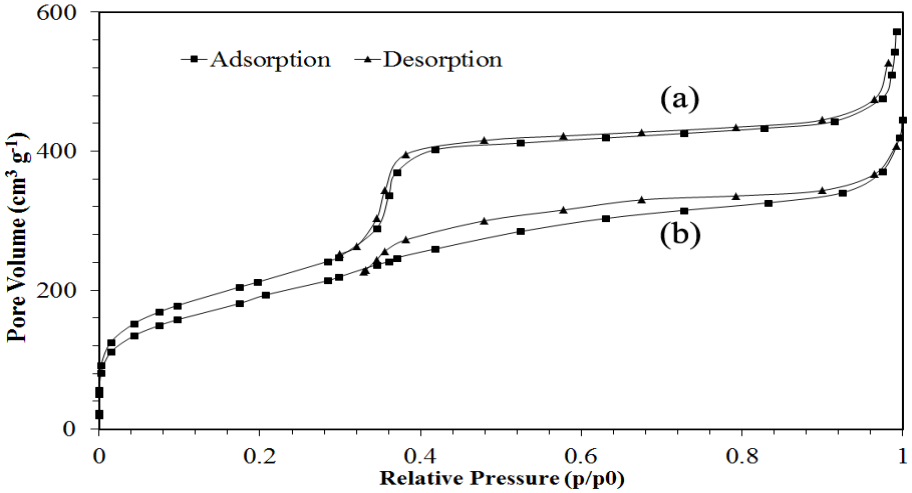

Fig. 6. The absorption-desorption diagram obtained from (a) mesoporous silica (MS) and (b) mesoporous silica containing benzotriazole (MSInh).

Figure 7 shows the impedance curve of resin/MS and resin/MSInh coatings in a solution of 0.03 M sodium chloride for during days. As can be seen, coatings containing inhibitor have a higher impedance modulus ($Z_{0.1}$ Hz) especially at 7-day and 10-day periods, which can be due to function of inhibitor containing benzotriazole in a corrosive solution and absorption on the steel and reduction of its corrosion rate. In the two mentioned time periods, the impedance modulus of the coating containing inhibitor is about 10 times more than the same type without inhibitor. Corrosion behavior of the coating at these times represents a time constant at the high frequencies related to the coating and a time constant related to the corrosion process. The effect of adsorption of benzotriazole on the surface and the reduction of available sites for corrosive ions can be considered the reasons of the higher resistance of the coatings with inhibitor. The benzotriazole release may also be considered by the repulsion of the zeta potential of the mesoporous silica surface. Mesoporous silica particles have a negative charge at alkali pH values [19], which results in the removal of benzotriazole inhibitor that also has a negative charge in the substrate and protects it.

The circuit models used to fit electrochemical impedance data is shown in Figure 8, in which R_s, R_c, R_{corr}, and CPE represent the solution resistance, coating resistance, charge transfer resistance (corrosion resistance), and constant phase element, respectively. CPE which displays the non-ideal capacitance in terms of constant phase element is given by $Z_{CPE} = 1/[T(j\omega)^n]$, where ω is the angular frequency, T and n are frequency-independent fit parameters, $j = (-1)^{1/2}$, and $\omega = 2\pi f$, where f is the frequency (Hz) [28-30]. According to the fitted results tabulated in Table 1, MSInh/resin had the greater R_{corr} and R_{coat} values than MS/resin which could be related to the gradual release of the corrosion inhibitor from MSInh nanocontainers and the barrier feature of the inorganic mesoporous silica particles. For example, after 10 days of immersion, the R_{corr} for MSInh/resin was 9×10^3 Ω cm^2, about 6 times greater than the corresponding value for MS/resin. R_{coat} values for MSInh/resin and

MS/resin were also 8×10^3 and 10^3 Ω cm^2, respectively. However, the penetration of the corrosive electrolyte into the coatings during the immersion resulted in a decrease in the corrosion resistance (R_{corr}) and coating resistance (R_{coat}) values of both MSInh/resin and MS/resin coating [31, 32]. Furthermore, by passing time, MSInh/resin and MS/resin coatings tended to have higher affinity towards ions and became more conductive. Therefore, any decrease in the R_{coat} values could be attributed to the accumulation of conductive species in the coatings [33, 34]. Besides, the lower CPE_{dl} for E/MSInh than E/MS indicates the higher corrosion resistance of the coating containing benozotriazole loaded mesoporous silica particles.

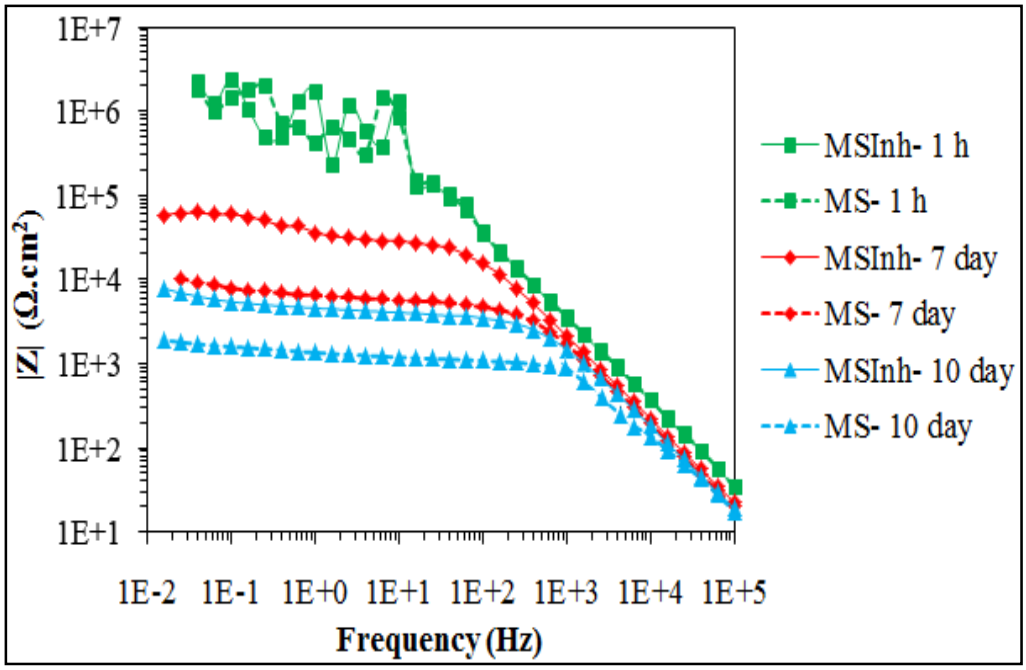

Fig. 7. Bode magnitude plot of MS/resin and MSInh/resin coatings in saline solution.

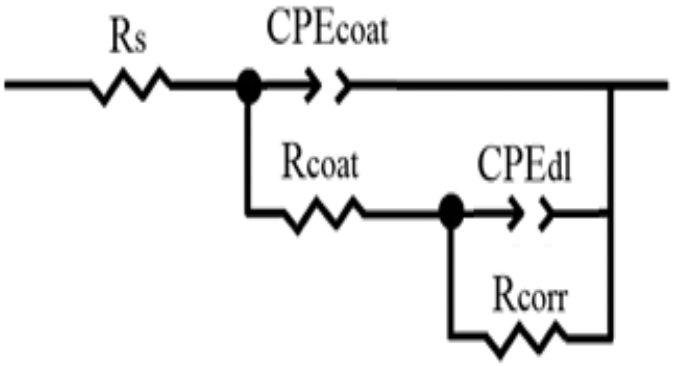

Fig. 8. Equivalent circuit regarding MS/resin and MSInh/resin coatings in saline solution.

Table 1. Electrochemical parameters obtained from EIS analysis of MSInh/resin and MS/resin coatings immersed for 10 days in 0.03 M NaCl solutions.

Sample	Time, day	R_{coat}, $\Omega\ cm^2$	CPE_{coat}, $F\ cm^{-2}\ s^n$	R_{corr}, $\Omega\ cm^2$	CPE_{dl}, $F\ cm^{-2}\ s^n$
MS/resin	1	10^5	3.5×10^{-5}	1.2×10^6	1.3×10^{-5}
	7	10^4	2.1×10^{-5}	3.1×10^4	2.2×10^{-4}
	10	10^3	4×10^{-4}	1.5×10^3	6.3×10^{-4}
MSInh/resin	1	1.2×10^5	1.3×10^{-5}	2.1×10^6	1.2×10^{-5}
	7	5×10^4	2×10^{-5}	1.2×10^5	1.4×10^{-4}
	10	8×10^3	1.2×10^{-5}	9×10^3	2.5×10^{-4}

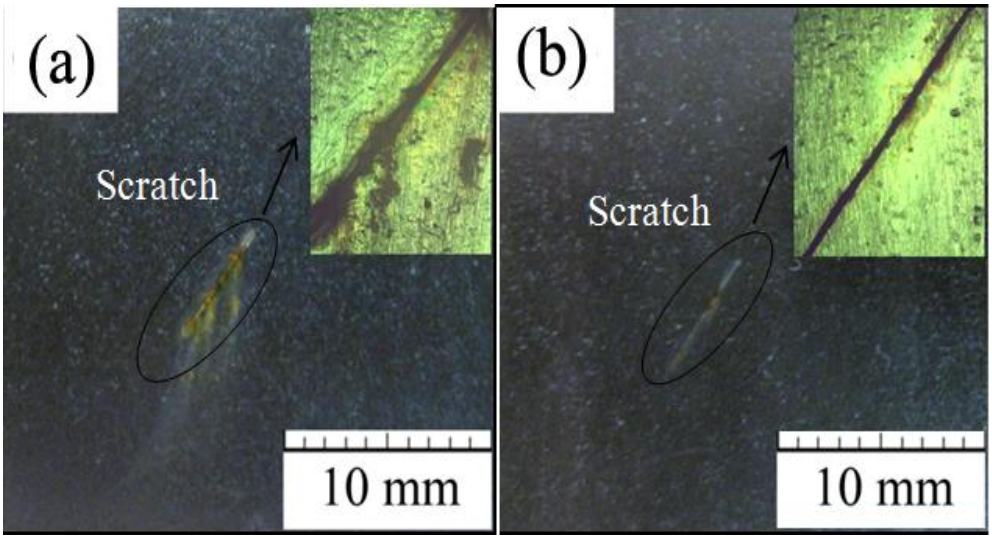

Fig. 9. The corrosion image of the (a) resin/MS and (b) resin/MSInh coatings after corrosion in chloride solution.

Figure 9 (a) and (b) shows the images of resin/MS and resin/MSInh coatings after 1 week of corrosion. As it can be seen, the corrosion products formed on the surface of a coating without inhibitor are more which are due to the direct availability of metal against a corrosive solution. The benzotriazole healing property was not sufficient to close the scratched area, but by the formation of a thin and discrete layer, it prevented the direct effect of the corrosive solution on the substrate.

4- Conclusion

In this study, the effect of benzotriazole inhibitor in the structure of mesoporous silica has been investigated in order to control the corrosion behavior of steel substrate. The results of the electrochemical impedance test showed that the inoculation of these particles within the coating increases the inhibitory property against the corrosive environment. SEM image also showed the formation of a layer by the benzotriazole inhibitor in the scratched area of

the coating, which in addition to its healing effect, increased the corrosion resistance of the system. Finally, this system can be considered as a smart corrosion resistant system that has higher corrosion resistance than the control sample by increasing pH value or scratching.

References

[1] Khramov, A. N., et al. "Sol–gel-derived corrosion-protective coatings with controllable release of incorporated organic corrosion inhibitors." Thin Solid Films 483.1 (2005): 191-196.

[2] Khramov, A. N., et al. "Hybrid organo-ceramic corrosion protection coatings with encapsulated organic corrosion inhibitors." Thin solid films 447 (2004): 549-557.

[3] Abdullayev, Elshad, and Yuri Lvov. "Clay nanotubes for corrosion inhibitor encapsulation: release control with end stoppers." Journal of Materials Chemistry 20.32 (2010): 6681-6687.

[4] Williams, G., S. Geary, and H. N. McMurray. "Smart release corrosion inhibitor pigments based on organic ion-exchange resins." Corrosion Science 57 (2012): 139-147.

[5] Deya, C., R. Romagnoli, and B. Del Amo. "A new pigment for smart anticorrosive coatings." Journal of Coatings Technology and Research 4.2 (2007): 167-175.

[6] Snihirova, D., et al. "Hydroxyapatite microparticles as feedback-active reservoirs of corrosion inhibitors." ACS applied materials & interfaces 2.11 (2010): 3011-3022.R. G. Buchheit, H. Guan, S. Mahajanam, F. Wong, Prog. Org. Coat. 47 (2003) 174–182.

[7] Buchheit, Rudolph G., et al. "Active corrosion protection and corrosion sensing in chromate-free organic coatings." Progress in Organic Coatings 47.3 (2003): 174-182.

[8] Shchukin, Dmitry G., et al. "Layer-by-Layer assembled nanocontainers for self-healing corrosion protection." Advanced Materials 18.13 (2006): 1672-1678.D.

[9] Andreeva, Daria V., Ekaterina V. Skorb, and Dmitry G. Shchukin. "Layer-by-layer polyelectrolyte/inhibitor nanostructures for metal corrosion protection." ACS Applied Materials & Interfaces 2.7 (2010): 1954-1962.

[10] V. M. Walczak, "Release studies on mesoporous microcapsules for new corrosion protection systems", Ruhr-Universität Bochum 2007.

[11] Yokoi, Toshiyuki, Takashi Tatsumi, and Hideaki Yoshitake. "Fe 3+ coordinated to amino-functionalized MCM-41: an adsorbent for the toxic oxyanions with high capacity, resistibility to inhibiting anions, and reusability after a simple treatment." Journal of colloid and interface science 274.2 (2004): 451-457.

[12] El-Sa, S. A. "y, A. Shahat, M. Mekawy, H. Nguyen, W. Warkocki and M. Ohnuma." Nanotechnology 21 (2010): 375603.

[13] She, Lan, et al. "High-resolution electron microscopy study of mesoporous dichalcogenides and their hydrogen storage properties." Nanotechnology 22.7 (2011): 075702.

[14] Zhu, Yufang, Jianlin Shi, Weihua Shen, Hangrong Chen, Xiaoping Dong, and Meilin Ruan. "Preparation of novel hollow mesoporous silica spheres and their sustained-release property." Nanotechnology 16, no. 11 (2005): 2633-2638.

[15] Zhao, Dongyuan, Yang Peidong, and Huo Qisheng. "Topological construction of mesoporous materials." Current Opinion in Solid State and Materials Science 3.1 (1998): 111-121.

[16] Rana, Rohit Kumar, Yitzhak Mastai, and Aharon Gedanken. "Acoustic cavitation leading to the morphosynthesis of mesoporous silica vesicles." Advanced Materials 14.19 (2002): 1414-1418.

[17] Slowing, Igor I, "Mesoporous silica nanoparticles for drug delivery and biosensing applications." Advanced Functional Materials 17.8 (2007): 1225-1236.

[18] Weiping, Cai, and Zhang Lide. "Synthesis and structural and optical properties of mesoporous silica containing silver nanoparticles." Journal of Physics: Condensed Matter 9.34 (1997): 7257-7267.

[19] Borisova, Dimitriya, Helmuth Möhwald, and Dmitry G. Shchukin. "Mesoporous silica nanoparticles for active corrosion protection." ACS nano 5.3 (2011): 1939-1946.

[20] Chen, Tao, and JiaJun Fu. "pH-responsive nanovalves based on hollow mesoporous silica spheres for controlled release of corrosion inhibitor." Nanotechnology 23 (2012): 235605.

[21] M. Saremi, M, Yeganeh, Application of mesoporous silica nanocontainers as smart host of corrosion inhibitor in polypyrrole coatings, Corros. Sci. 86 (2014) 159–170.

[22] V. von, "Release studies on mesoporous microcapsules for new corrosion protection systems", Ph.D. thesis, 2007, Bochum University.
[23] Y. Huang, Ph.D. Thesis, "Functionalization of mesoporous silica nanoparticles and their applications in organo- metallic and organometallic catalysis" Iowa State University, (2009). Page 8.
[24] S. Tamil Selvi, V. Raman, N. Rajendran, "Corrosion inhibition of mild steel by benzotriazole derivatives in acidic medium", Journal of Applied Electrochemistry 33 (2003) 1175-1182.
[25] X. Wang, P. Wang, Z. Dong, Z. Dong, Z. Ma, J. Jiang, R. Li, J. Ma, Highly Sensitive Fluorescence Probe Based on Functional SBA-15 for Selective Detection of Hg^{2+}", Nanoscale. Research. Lett. 5 (2010) 1468–1473.
[26] J. Lu, Y. Li, C. Deng, Facile synthesis of zirconium phosphonate-functionalized magnetic mesoporous silica microspheres designed for highly selective enrichment of phosphopeptides, Nanoscale 3 (2011) 1225–1233.
[27] Z. A. ALOthman, "A Review: Fundamental Aspects of Silicate Mesoporous Materials", Materials 5 (2012) 2874-2902.
[28] A. Keyvani, M. Yeganeh, H Rezaeyan, Electrodeposition of Zn-Co-Mo alloy on the steel substrate from citrate bath and its corrosion behavior in the chloride media, J. Mater. Eng. Perform. 26 (2017) 1958-1966.
[29] M. Yeganeh, M. Eskandari, S. R. Alavi-Zaree, A Comparison Between Corrosion Behaviors of Fine-Grained and Coarse-Grained Structures of High-Mn Steel in NaCl Solution, J. Mater. Eng. Perform. 26 (2017) 2484-2490.
[30] M. Eskandari, M. Yeganeh , M. Motamedi , Investigation in the corrosion behaviour of bulk nanocrystalline 316L austenitic stainless steel in NaCl solution, Micro and Nano Letters, 7 (2012) 380 – 383.
[31] A. Keyvani, M. Yeganeh, H. Rezaeyan, Application of mesoporous silica nanocontainers as an intelligent host of molybdate corrosion inhibitor embedded in the epoxy coated steel, Prog. Nat. Sci. Mater. Int. 27 (2017) 261–267.
[32] M. Saremi, M.Yeganeh, Corrosion behavior of copper thin films deposited by EB-PVD technique on thermally grown silicon dioxide and glass in hydrochloric acid media, Mater. Chem. Phys. 123 (2010) 456-462.
[33] Yeganeh, M., and A. Keyvani. "The effect of mesoporous silica nanocontainers incorporation on the corrosion behavior of scratched polymer coatings." Progress in Organic Coatings 90 (2016) 296-303.
[34] M. Yeganeh, N. Asadi, M. Omidi, M. Mahdavian, An investigation on the corrosion behavior of the epoxy coating embedded with mesoporous silica nanocontainer loaded by sulfamethazine inhibitor, Prog. Org. Coatings. 128 (2019) 75-81.